Population Balance Modeling of a Microalgal Culture in Photobioreactors: Comparison Between Experiments and Simulations

Alberto Bertucco, Eleonora Sforza, Valentina Fiorenzato, and Matteo Strumendo
Dept. of Industrial Engineering DII, University of Padova, Via Marzolo 9, 35131 Padova, Italy

DOI 10.1002/aic.14893
Published online August 7, 2015 in Wiley Online Library (wileyonlinelibrary.com)

The growth of Scenedesmus obliquus *in photobioreactors was both experimentally investigated and numerically simulated by solving a population balance equation (PBE), accounting for cell growth and division. The PBE is solved using the Finite size domain Complete set of trial functions Method Of Moments (FCMOM) and a wide range of operative conditions, namely both a batch and a continuous reactor under different light intensities, were considered in the experiments and in the numerical simulations. A thorough validation of the mathematical model was performed by comparing the experimental temporal profiles and steady-state values of the cell density, wet weight, cell average mass, and mass distributions of the microalgal culture with the corresponding simulation results. The parameters of the distribution of division mass were identified to fit the experimental data; specifically, from the continuous reactor data, the dependence of the mean division mass from the cell average mass was obtained.* © 2015 American Institute of Chemical Engineers *AIChE J*, 61: 2702–2710, 2015
Keywords: Scenedesmus obliquus*, growth modeling, single cell mass, light intensity*

Introduction

Currently, about 90% of energy is generated from fossil fuels and only about 10% is produced from renewable energy sources.[1] The energy demand is continually increasing and the research of alternative renewable sustainable energy sources is no longer an option. Microalgae have a high potential for producing biomass which in turn can be used for the production of different third-generation biofuels at large scale.[1]

The commercial exploitation of microalgae for sustainable biofuel faces several challenges due to low productivity, high cost, and technical issues.[2,3]

The major limitation of a successful biofuel production from photosynthetic organisms is the absence of effective engineering strategies and a suitable operation approach for microalgae-based biofuel production. In this context, continuous processes may be suitable for large-scale cultivation of microalgae for industrial applications because they are generally more productive, low cost, and easy to operate than batch cultures.[2]

Understanding the biomass properties is essential for monitoring and controlling biotechnological processes, particularly in continuous biological reactors. Generally, the control of bioprocesses is restricted to some physical and chemical parameters, such as pH value or temperature,[4] and the biological biomass has been considered as a "homogeneous catalyst." However, in a bioreactor, cells are not identical, but constitute a heterogeneous population described by a distribution of cell states: the state of a cell can be cell mass, size, age, and biochemical composition.[5–7] This heterogeneity may originate from stochastic gene transcription, translation and regulation, differences in progression through cell cycle phases, and by an unequal cell division which implies a different lifetime for each daughter cell.[5,7,8]

The heterogeneity of cell populations can be accounted for through population balance modelling.[9,10] In fact, population balance equations (PBEs) were developed to mathematically describe and predict the dynamics of populations of entities (cells, but also particles, droplets, etc.). In population balance modelling, one or more internal variables are selected to define the state of the entities, which are characterized in terms of a distribution function of the internal variables. The PBEs describe the temporal and spatial evolution of such internal variable distribution function.

In the case of cell populations, the internal variable used to define the cell physiological state has been frequently the cell mass[7,9,11] but other internal variables, such as the cell age or the cell volume, have been considered as well.[9,10,12] The advantages of using the population balance modeling over the "homogeneous catalyst" approach include:

1. the cell growth rate dependence on the cell mass is taken into account[11,13];
2. a cell division model, dependent on the internal variables, can be included in the PBE, thus providing the information required to monitor the variation in the cell number density over time and/or space.

According to the current literature on biological heterotrophic processes, the existence of different spatial microenvironments within a reactor may imply differential responses of cells and this fact has been suggested as the main underlying

Correspondence concerning this article should be addressed to Alberto Bertucco at alberto.bertucco@unipd.it

cause for differences between cultivations performed in well-mixed lab scale bioreactors and more poorly mixed large-scale reactors[6,14]: for instance, in the case of heterotrophic cultures, cells appear to be affected by the substrate concentration that induces modifications of the cell metabolism and causes a decrease in the overall reactor performance.[15]

Similarly, for photosynthetic organisms, light irradiance plays a key role in photosynthesis and thereby strongly influences the growth and cell composition of photoautotrophic microalgae.[16] Under phototrophic conditions, the increasing turbidity associated with the increase of microalgal concentration usually becomes a significant growth-limiting factor due to the self-shading effect.[2] Thus, the light distribution in a photobioreactor (PBR) may result in different microenvironments where light limitation, light saturation, or light inhibition can occur.[17]

Even though PBEs have been frequently used to model/simulate the dynamics of cell populations, to the best of our knowledge few contributions are available in literature on the application of PBEs to photosynthetic organisms.[11,12,18] In particular, Concas et al.[11] proposed a PBE model, based on the cell mass as internal variable, to simulate the growth of microalgae in BIOCOIL PBRs, taking into account the light intensity distribution within the reactor. They performed transient simulations assuming an initial gaussian cell mass distribution function, obtaining the trends of the nutrient/oxygen concentrations, of the photosynthetically active radiation (PAR) and of the cell mass distribution over time and reactor length. The biomass concentration and average mass trends over time at the last section of the tube were computed from the cell mass distribution. The latter (average cell mass at the tube last section) showed an oscillatory behavior, the former (biomass concentration at the tube last section) increased monotonically until the nutrients were consumed and was the only quantity compared with experimental data.[19] Altimari et al.[18] used a bivariate PBE using mass and age as internal variables to simulate a PBR, but no comparison with experimental data was provided. In conclusion, even though the mentioned contributions demonstrate the potential predictive capabilities of the PBEs applied to PBRs, a convincing validation of such models through a detailed comparison with experimental data has not been carried out thus far.

In this work, a thorough validation of a PBE model accounting for the cell growth and cell division of a microalgal culture in PBRs is carried out by comparing the simulation results with experimental data of cell number density, wet weight, cell average mass size, and cell mass distributions measured both in a batch and in a continuous PBRs. The mathematical model, based on cell mass as internal variable, takes into account the effects of the light intensity distribution and of the substrate concentrations within the PBRs and was numerically solved through the FCMOM technique.[20]

The microalgae *Scenedesmus obliquus*, an organism of widely recognized biotechnological interest and a potential candidate for biodiesel production[1,21,22] was used in the experimental measurements. Additionally, values of the parameters (mean and standard deviation) of the distribution of division mass, required to evaluate the cell division terms in the PBE, were identified from the experimental data fit. Thus, differently than previous contributions[11] in which reasonable/typical values were used, in this work values of such parameters specific of photosynthetic microalgae are provided.

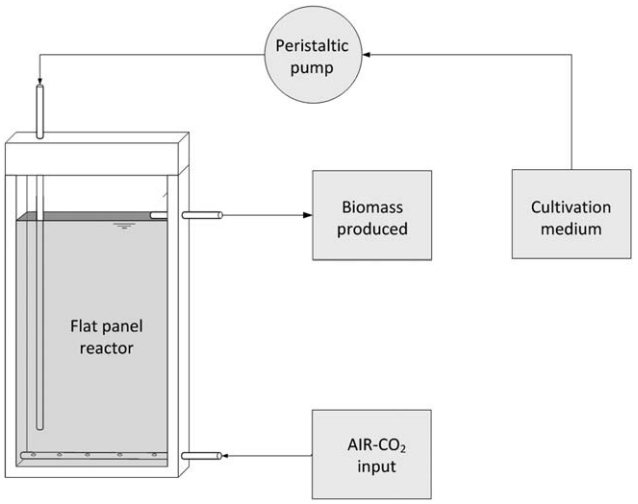

Figure 1. Schematic of the continuous flat panel reactor.

Materials and Methods

Species and growth medium

The microalgal species *Scenedesmus obliquus* 276-7 (from SAG-Goettingen) was cultured in BG11 medium, buffered with 10 mM HEPES pH 8, to avoid acidification due to CO_2 bubbling. The medium was sterilized in an autoclave for 20 min at 121°C to prevent any contamination, as well as all the reactor and materials. All nutrients were provided in nonlimiting concentration, in the case of continuous experiments, with particular attention to macronutrients: the P and N content of the medium were optimized to avoid nutrient limitation in continuous experiments, with a concentration of 3 g L^{-1} and 0.56 g L^{-1} of $NaNO_3$ and K_2HPO_4, respectively.

Equipment and experimental procedures

Growth experiments were performed both in batch and continuous conditions, in vertical flat-plate polycarbonate PBRs (a detailed schematic of the experimental set up is presented in Figure 1), with a thickness of 12 mm. The working reacting volumes of the batch and continuous panels are 150 mL and 400 mL, respectively. In both cases, the mixing in the culture is ensured by a CO_2–air (5% v/v) flow at the reactor bottom (1 L h^{-1} of total gas flow rate for each panel), that also provided a nonlimiting CO_2 supply. In the case of continuous reactor, an additional magnetic stirring was added. This system can be approximated to a Continuous Stirred Tank Reactor (CSTR), as demonstrated by tracer experiments.[23]

Batch experiments were carried out by inoculating the biomass at optical density (OD_{750}) of 0.1 as initial value, measured by a spectrophotometer UV-Visible (UV 500, Spectronic Unicam, UK). In the continuous system, the reactor was started first in batch mode to reach a higher concentration (about 10^8 cell mL^{-1}) and to prevent the occurring of washout. Subsequently, the operation was switched to continuous, by feeding the medium with a peristaltic pump (Sci-Q 400, Watson Marlow, USA) from a tank, continuously mixed with a magnetic stirrer and maintained at the same temperature of the reactor. The liquid level in the reactor was controlled with an overflow tube, and the outlet flow rate was collected in a bottle. Thus, the residence time in the reactor was directly controlled by the peristaltic pump. Several flow rates were used,

leading to different residence times. Transient conditions were observed after each change, then steady-state operation was reached and maintained at least for 4–7 days. Light was provided by a LED lamp (Photon System Instruments, SN-SL 3500-22). Two batch experiments were carried out, under constant light intensities of 150 e 350 μmol of photons m^{-2} s^{-1}. In the continuous experiment microalgal growth was studied under 150 μmol m^{-2} s^{-1} and different residence times. Photon Flux Density was measured on both the reactor front panel and on the back of the rear one using a photoradiometer (HD 2102.1 from Delta OHM), which quantifies the PAR.

Growth analysis

The biomass concentration of batch experiments was monitored daily by spectrophotometric analysis of the OD, correlated to cell number density, measured with a Bürker Counting Chamber (HBG, Germany) as detailed by Gris et al.[21] The concentration of biomass was also gravimetrically measured every day as dry weight (DW) in terms of g L^{-1} in cells harvested with a 0.22 μm filter, and then dried for 4 h at 80°C in a laboratory oven. In continuous experiments, cell concentration and DW were monitored daily and the steady-state concentrations were averaged over three to five experimental points.

Cell size distributions were measured by the Cellometer Auto X4 (Nexcelon Bioscience), a PC-based automated cell counter. This instrument utilizes bright field imaging, fluorescent imaging, and pattern-recognition software to provide cell count in terms of number, concentration, size, and viability of cells.

A single cell density of 1.2 g mL^{-1} was considered for *S. obliquus* as an averaged value of weight measures under different growth conditions. A spherical shape of cells was assumed, by considering that *S. obliquus* do not grow as coenobia in our experimental conditions, that is, where an excess of CO_2 is provided to the culture. This was confirmed both qualitatively (by optical microscope observation) and quantitatively (by counts at the cellometer).

Basing on single cell density and cell size measured by the cellometer, it is possible to derive the cell mass distribution. From cell mass distribution, the averaged mass of a single cell and the concentration of wet biomass or wet weight in g L^{-1} can be easily calculated. The wet biomass concentration corresponds to the cell weight, including the intracellular water content, also considering the residual moisture content of 8% that remains in the DW.[24] Accordingly, the water content of the whole biomass resulted about 80%, which is in agreement with literature data.[25–27]

Mathematical Modeling and Numerical Approach

The governing equations used to model the microalga growth in the batch and continuous PBRs are based on the following assumptions:

1. the PBRs are operated in isothermal conditions and are well-mixed, therefore the only "external" coordinate[10] is time, *t*.
2. Two phases are included in the model, namely the solid pellet, described by a heterogeneous microalga population, and the liquid phase, where nutrients are dissolved. Instead, the gas phase is neglected in the present model.
3. The effect of the nutrient concentration on the cell growth is neglected in the continuous reactor. In fact, an excess of micro and macro nutrients (specifically N-NO_3 and P-PO_4) is fed in this case, therefore, they are not limiting nutrients (as detailed in Section Materials and Methods).
4. The reactor liquid level can be assumed constant and no cells are fed into the photobioreactors (Section Materials and Methods).
5. Cell division is assumed to be binary.
6. Cell death is assumed to be negligible, as resulting from experimental observations obtained with the cellometer, namely the fraction of living cells, provided by the cellometer for fresh samples, is always higher than 90%.

The governing equations, based on the above assumptions, used to simulate the microalga growth can be divided in:

1. the population balance model required to simulate the cell population dynamics;
2. the mass balances of the limiting nutrients (for the batch PBR);
3. an equation providing the light intensity distribution within the PBRs.

Population balance model

The internal variable used to define the physiological state of the microalgae is the mass *m* and the cell mass distribution function is denoted by *W(t,m)*. It is assumed that the mass domain is bounded between zero and a maximum mass m_{max}[20,28]; in this work such maximum value is kept constant with respect to time. The PBE governing the temporal evolution of the cell mass distribution is then formulated as follows[20,28,29]

$$\frac{\partial W(t,m)}{\partial t}+\frac{\partial r(t,m)W(t,m)}{\partial m} = 2\int_{m}^{m_{max}} p(m,m')\Gamma(t,m')W(t,m')dm'-\Gamma(t,m)W(t,m)-D(t)W(t,m) \quad (1)$$

In Eq. 1, on the left-hand side there are the accumulation term and the contribution due to the cell growth; *r(t,m)* is the single-cell growth rate. On the right-hand side, there are the terms of cell birth and death due to binary division and the washout term (at the continuous reactor outlet); Γ is the division intensity, *p* is the partition probability density function, and *D* is the dilution rate, assumed to be equal to the volumetric flow rate divided by the culture volume.[29]

The single-cell growth rate *r(t,m)* is expressed through the following expression (linear with respect to the cell mass), accounting both for effect of the light and of the nutrients

$$r(t,m)=\left\{k_{max}\frac{C_P(t)}{k_{mP}+C_P(t)}\frac{C_N(t)}{k_{mN}+C_N(t)}\frac{1}{H}\left[\int_0^H\frac{I_{dir}(t,h)}{k_{mI}+I_{dir}(t,h)}dh\right]-k_p\right\}m \quad (2)$$

In Eq. 2, k_{max} is the maximum specific cell growth rate, k_p is the catabolic growth rate, k_{mP} and k_{mN} are the half saturation constants for the nutrients (K_2HPO_4 and $NaNO_3$, respectively), k_{mI} is the light half-saturation constant, C_P and C_N are the mass concentrations of the nutrients (K_2HPO_4 and $NaNO_3$ respectively), I_{dir} is the direct contribution to the PAR in the culture varying along the reactor depth *h*,[30,31] and *H* is the reactor thickness. The contributions of the nutrients are equal to unity and are neglected for the continuous reactor, which is fed by an excess of nutrients.

The maximum specific cell growth rate is computed as $k_{max}=\rho_m k_{mI}\Phi E_a$, ρ_m being the maximum energy yield for

photon dissipation in the antenna, Φ being the mean spatial quantum yield for the Z-scheme of photosynthesis, and E_a being the absorption mass coefficient. The division intensity is modeled according to Eakman et al.[7]

$$\Gamma(m,t)=\frac{2r(t,m)\exp\left[-\left(\frac{m-m_c}{\varepsilon}\right)^2\right]}{\varepsilon\sqrt{\pi}\left[1-\mathrm{erf}\left(\frac{m-m_c}{\varepsilon}\right)\right]} \tag{3}$$

In Eq. 3, m_c and $\frac{\varepsilon}{\sqrt{2}}$ are, respectively, the mean and the standard deviation of the distribution of division mass.

The partition probability density function describes how mass is distributed between daughter cells at division and is expressed through the following equation[29]

$$p(m,m')=30\frac{m^2(m'-m)^2}{m'^5} \tag{4}$$

Mass balance of nutrients

The mass balances of the nutrients are used for the batch reactor simulations. They account for the accumulation and consumption terms, according to the following equation[29]

$$\frac{dC_j(t)}{dt}=-\int_0^{m_{\max}}\frac{r(t,m)W(t,m)}{y_j}dm \tag{5}$$

In Eq. 5, the index j refers to the nutrient considered (P-PO_4 and N-NO_3) and y_j are the nutrient yields (rate of biomass formation over rate of nutrient consumption).

PAR spatial distribution

Pruvost et al. (2011) provided an expression to compute the spatial (along the reactor depth) distribution of the direct (collimated) contribution to the PAR[31]

$$I_{\mathrm{dir}}(t,h)=I_{\mathrm{dir}}(t,0)\frac{2}{\cos\vartheta}\frac{(1+\alpha)\exp[-\delta_{\mathrm{dir}}(t)(h-H)]-(1-\alpha)\exp[\delta_{\mathrm{dir}}(t)(h-H)]}{(1+\alpha)^2\exp[\delta_{\mathrm{dir}}(t)H]-(1-\alpha)^2\exp[-\delta_{\mathrm{dir}}(t)H]} \tag{6}$$

According to Pruvost et al.,[30] in Eq. 6 the two-flux direct extinction coefficient is given by

$$\delta_{\mathrm{dir}}(t)=\frac{\alpha C_X(t)(E_a+2bE_s)}{\cos\vartheta} \tag{7}$$

and the linear scattering modulus is given by

$$\alpha=\sqrt{\frac{E_a}{E_a+2bE_s}} \tag{8}$$

In the previous equations, E_a and E_s are the absorption and backscattering mass coefficients, b is the backscattered fraction, C_X is the dry biomass concentration, and ϑ is the incident angle with respect to the perpendicular to the reactor surface.

Numerical approach

The PBE (1) was solved through the FCMOM technique.[20] According to such technique, after recasting the mass domain into the domain $[-1,1]$ using the transformation

$$\overline{m}=2\frac{m}{m_{\max}}-1 \tag{9}$$

a dimensionless cell mass distribution is defined as $\overline{W'(t,\overline{m})}=\frac{W(t,m)}{W_{sc}}$, W_{sc} being an arbitrary scale factor (in the simulations discussed in Section Results and Discussion, the peak value of the initial cell mass distribution is used as scale factor). The dimensionless moments are defined and computed by the following equation

$$\mu_i=\int_{-1}^{1}\overline{W'}(\overline{m})^i d\overline{m} \tag{10}$$

The dimensionless cell mass distribution is computed by a truncated series expansion

$$\overline{W'}(t,\overline{m})=\sum_{n=0}^{M-1}c_n(t)\phi_n(\overline{m}) \tag{11}$$

In the previous equation, the series expansion is truncated after M terms, $\phi_n(\overline{m})$ are the orthonormal functions associated to the Legendre polynomials, and the series coefficients are related to the dimensionless moments through the following equation

$$c_n=\sqrt{\frac{2n+1}{2}}\frac{1}{2^n}\sum_{v=0}^{n}(-1)^{n-v}\frac{(2v)!}{[(2v-n)!]}\left\{\frac{1}{[(n-v)!][(v)!]}\right\}\mu_{2v-n} \tag{12}$$

where the terms with negative moments are to be omitted. Therefore, the cell mass distribution is completely determined by the dimensionless moments.

The dimensionless moments governing equations provide the evolution of the moments over time.[20] The following dimensionless moments governing equations are obtained from the PBE (1)

$$\begin{aligned}&\frac{\partial\mu_i(t)}{\partial t}+\frac{2}{m_{\max}}\left[r(t,m=m_{\max})\overline{W'}(t,\overline{m}=1)\right.\\&\left.-i\int_{-1}^{1}r(t,m)\overline{W'}(t,\overline{m})(\overline{m})^{i-1}d\overline{m}\right]=\\&=\frac{2}{W_{sc}}\int_{-1}^{1}(\overline{m})^i\left[\int_{m}^{m_{\max}}p(m,m')\Gamma(t,m')W(t,m')dm'\right]d\overline{m}\\&-\int_{-1}^{1}\Gamma(t,m)\overline{W'}(t,\overline{m})(\overline{m})^i d\overline{m}-D(t)\mu_i(t)\end{aligned} \tag{13}$$

Equation 13 is obtained enforcing the conditions that the minimum mass (equal to zero) and maximum mass do not change with time and that the "cell flux" at the minimum mass is zero (namely, $r(t,m=0)W(t,m=0)=0$). Equation 13 is solved using Eq. 9, which provides the correspondence between cell mass and dimensionless cell mass (particularly, at the maximum cell mass the corresponding dimensionless value is 1). On the left-hand side, there are the moment accumulation rate and the contributions from the cell growth. On the right-hand side, there are the terms of birth/death of cells due to cell division and the washout term (at the continuous reactor outlet).

In the batch reactor simulations, initial conditions for the nutrient mass concentrations and for the dimensionless moments are required to solve the ordinary differential Eqs. 5 and 13. The initial nutrient mass concentrations are reported in Section Materials and Methods, and the initial conditions for the moments are computed from the initial experimental cell mass distribution using Eq. 10.

In the continuous reactor simulations, a method of false transients was used to obtain the stationary state solutions for a given value of the dilution rate D, that is, the residence time.

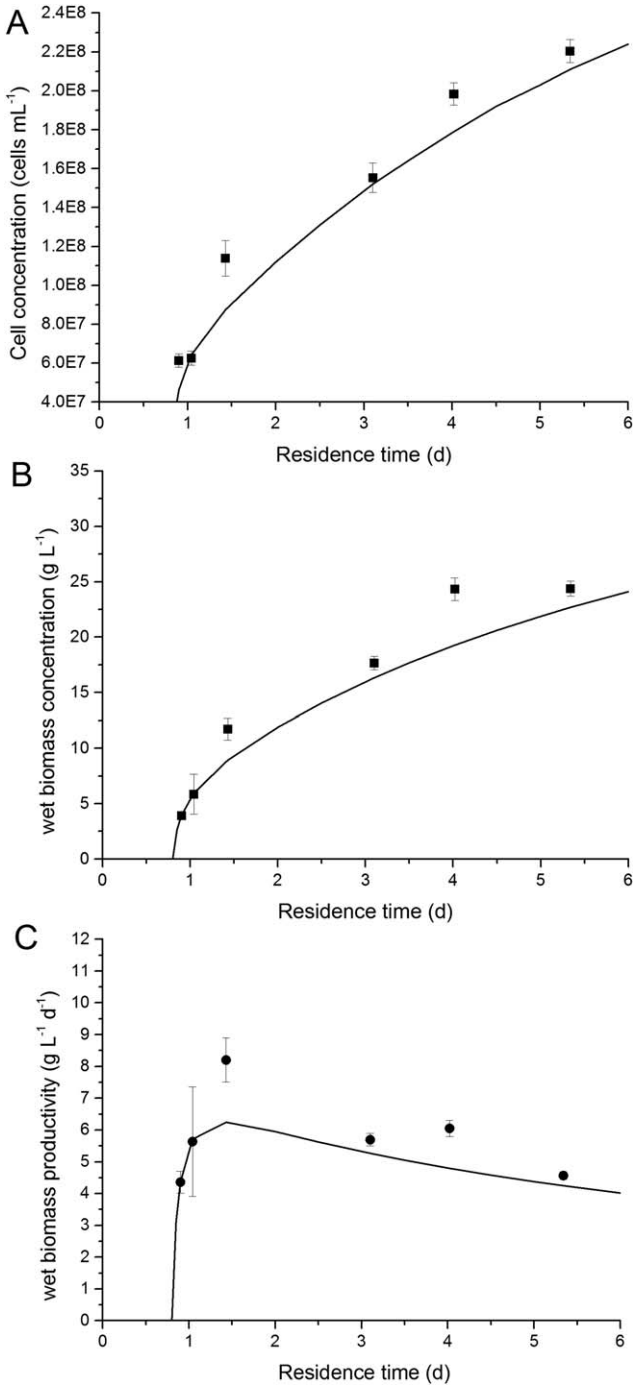

Figure 2. Cell number (A), wet biomass concentration (B) and productivity (C) for *S. obliquus* as a function of residence time.

Squares and dots represent the experimental data, while continuous lines are the output of the PBE model.

The cell number density N and the wet biomass concentration C_B are computed from the zeroth and first dimensionless moments through the following equations

$$N = \frac{m_{\max}}{2} W_{sc} \mu_0 \tag{14}$$

$$C_B = \left(\frac{m_{\max}}{2}\right)^2 W_{sc}(\mu_1 + \mu_0) \tag{15}$$

According to the experimental observations reported in Section Materials and Methods, the dry biomass concentration is computed from the wet biomass concentration using $C_X = 0.22 C_B$.

Results and Discussion

Continuous reactor experiments

Continuous reactor experiments were carried out in a flat panel, as reported in Section Materials and Methods, under a constant irradiation, and varying the inlet stream flow-rate, to investigate the effect of the residence time τ, equal to the inverse of the dilution rate D, on the cell growth. A transient stage of about 7 days was observed for each value of residence time selected before reaching the steady-state condition. This was verified by measuring a constant biomass concentration for at least 3–5 days. For each steady-state run (namely for each residence time) the N and P consumption were monitored, to check that the concentrations of such nutrients were nonlimiting, by measuring the N and P concentrations in the outlet stream. In Figure 2, the experimental measurements of the wet biomass concentration (in terms of g L^{-1}) and of the cell number density are plotted as a function of the residence time. As already reported by other authors,[32–34] both the biomass concentration and the cell number density increase when the residence time is increased. On the other hand, a maximum in productivity was found as a function of the residence time (Figure 2C), due to the higher self-shading of cells at higher residence times, which causes a decreasing productivity.[34] On the opposite, at low residence times, the biomass productivity drops because the reactor operates close to the washout value.[32,34]

The PBE model was solved for each value of the residence time and the obtained simulation results are shown in Figure 2 as well. The values used in the numerical simulations for the parameters required to compute the single-cell growth rate $r(t,m)$ are reported in Table 1. The parameters ρ_m, Φ, k_p are derived by Pruvost et al.,[30] while the values of the parameters E_a, bE_s, and k_{mI} specific for *Scenedesmus obliquus* were obtained by Sforza et al.[31] The parameters of nutrient consumption kinetics were not considered in the continuous reactor simulations, due to the excess of N and P provided to the culture. In all the numerical simulations of the continuous reactor, ε (parameter related to the standard deviation of the distribution of division mass) was assumed equal to 70 pg, while m_c (average of the distribution of division mass) was varied for each τ in order to fit the experimental data of wet biomass concentration and of cell number density. To the best of our knowledge, a comparison between experimental data of wet biomass concentration and cell number density as functions of τ and the corresponding simulation results obtained through a PBE model was never performed for a continuous PBR. Figure 2 shows that, by tuning m_c, a nice agreement between experimental data and simulation results was obtained, both for the wet biomass concentration and for the cell number density. The trend of the wet biomass productivity vs. residence time is captured as well by the simulations results (Figure 2C), both at low and high residence times, reproducing also the maximum in productivity.

Additionally, it was found that a linear relationship holds between the values of m_c (obtained to fit the experimental data) and the computed average cell mass $\langle m \rangle$, at each residence time. Such relationship was fitted through a straight line, namely

$$m_c = -9.40 + 1.57\langle m \rangle \tag{16}$$

which is plotted in Figure 3.

Table 1. Values of Parameters used in the PBE Model, in the Case of Continuous and Batch Simulations, Derived and Adapted from Literature, as Reported in Section Results and Discussion.

	Continuous 150	Batch 150	Batch 350
ρ_m	0.8	0.8	0.8
Φ	$2.77 \cdot 10^{-9}$ kg μmol^{-1}	$2.77 \cdot 10^{-9}$ kg μmol^{-1}	$2.77 \cdot 10^{-9}$ kg μmol^{-1}
E_a	170 m^2 kg^{-1}	170 m^2 kg^{-1}	150 m^2 kg^{-1}
bE_s	40 m^2 kg^{-1}	40 m^2 kg^{-1}	9 m^2 kg^{-1}
k_p	0.1 d^{-1}	0.1 d^{-1}	0.24 d^{-1}
k_{mI}	75 μmol m^{-2} s^{-1}	75 μmol m^{-2} s^{-1}	75 μmol m^{-2} s^{-1}
k_{mP}	–	0.27 mg$_P$ L^{-1}	0.27 mg$_P$ L^{-1}
$1/y_P$	–	$3.74 \cdot 10^{-4}$ mg$_P$ mg$_{biomass}^{-1}$	$2.67 \cdot 10^{-4}$ mg$_P$ mg$_{biomass}^{-1}$
k_{mN}	–	12.1 mg$_N$ L^{-1}	12.1 mg$_N$ L^{-1}
$1/y_N$	–	0.016 mg$_N$ mg$_{biomass}^{-1}$	0.0115 mg$_N$ mg$_{biomass}^{-1}$

It was also obtained from the simulation results that the average cell mass increases monotonically with the residence time. This is confirmed also by data reported in Sforza et al.[34] about the average cell mass in continuous PBR, which shows a decreasing trend when the specific growth rate increases, namely when the residence time decreases.

Batch reactor experiments

In the case of batch reactor, the simulated data were compared with the experimental ones, under two irradiation values of 150 and 350 μmol m^{-2} s^{-1}, obtained by measuring daily the cell concentration, the DW and the cell mass distribution. An optimal value of light intensity for this species is 150 μmol m^{-2} s^{-1}, at which the specific maximum growth rate can be achieved, as already observed by Gris et al.[21] In fact, as shown in Figure 4, no lag phase was detected and the cell culture grew with an initial exponential phase of about 4–5 days, suggesting that cells are well adapted to this optimum light condition. Afterward, a stationary phase was reached, where no increase of biomass was observed. In batch microbial growth curves, the establishment of a stationary phase is a common behavior, usually due to the gradual depletion of some nutrient, which is consumed by the growing biomass. In the case of photosynthetic organisms, a stationary phase can also be reached by a light limitation that can occur under high cell concentration, resulting in an increased self-shading effect.

This batch experiment was simulated by applying the parameter values reported in Table 1, which are the same as for the continuous reactor. In this case, however, the kinetics of nutrient uptake is taken into account, because macronutrients, even though are provided in excess at the beginning of the experiment (and therefore have no effect on the growth kinetics at the beginning of the experiment) are consumed over time as a result of the biomass growth and become factors limiting the cell growth during the batch experiment. The values of the parameters k_{mP}, k_{mN}, $1/y_P$, and $1/y_N$ were calculated from the nutrient consumption and biomass productivity measured in the experimental part of this work, and were found in good agreement with data retrieved from literature.[35] In

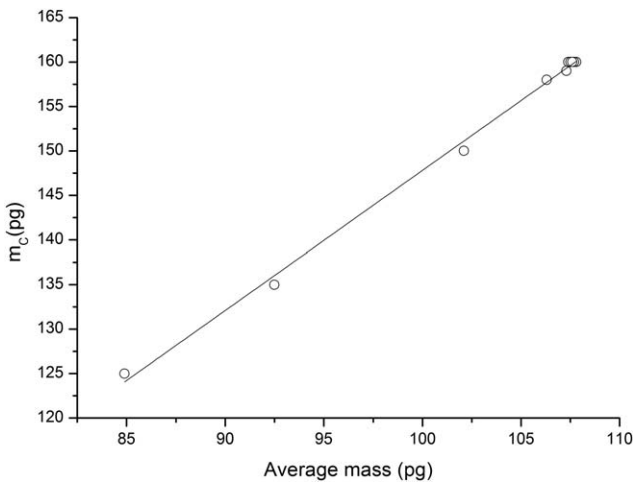

Figure 3. Linear correlation between the m_c parameter value and the average mass of the culture.

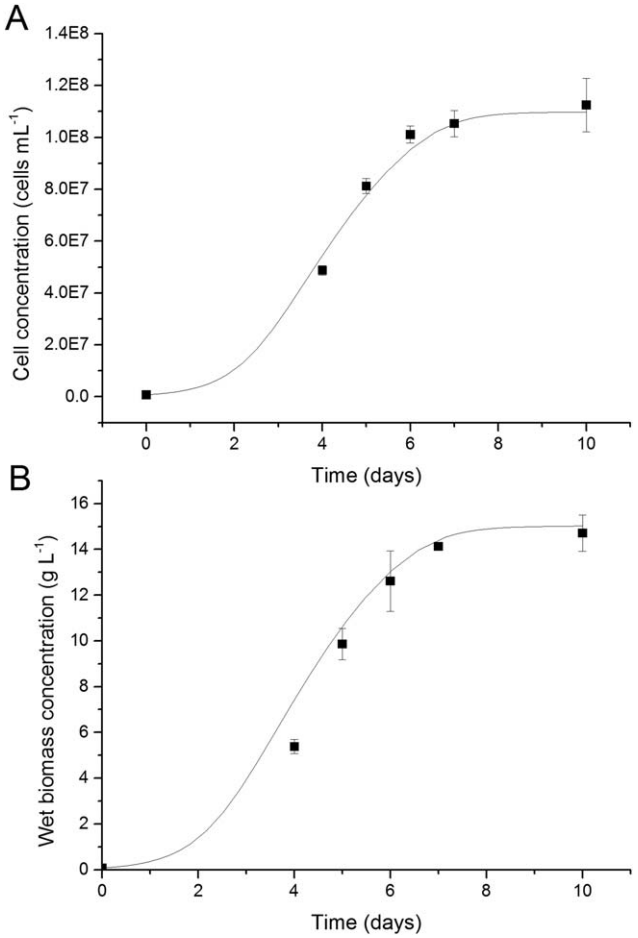

Figure 4. Cell (A) and wet biomass (B) concentrations for *S. obliquus* in batch experiment carried out under 150 μmol of photons m^{-2} s^{-1}.

Squares represent the experimental data, while continuous lines are the results of the PBE model.

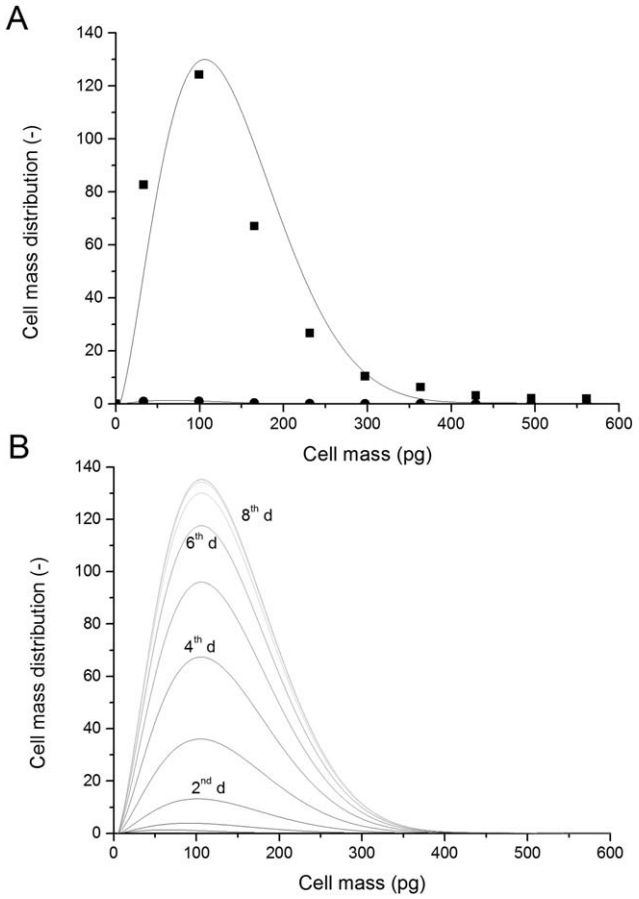

Figure 5. In Figure 5A experimental cell mass distribution of the first (dots) and seventh (squares) day of growth of *S. obliquus* in batch experiment carried out under 150 μmol of photons m^{-2} s^{-1}, compared with the simulated ones (solid lines) are reported.

Figure 5B shows the simulated distribution of cell mass up to the eighth day.

addition, the parameter m_c was computed as a function of the average cell mass through the linear relationship developed for the continuous reactor (Eq. 16). Instead, the only parameter which has a different value in the batch reactor simulations (with respect to the corresponding value in the continuous reactor simulations) is ε (parameter related to the standard deviation of the distribution of division mass): a constant value of 120 pg was selected for ε, in order to fit the experimental data of cell number density and of wet weight vs. time. The simulation results show that the PBE model used is capable to represent with a satisfactory approximation the experimental data of both cell number density and wet weight, not only under stationary conditions but also in a dynamic batch reactor (Figure 4B).

A nice agreement between the experimental and calculated cell mass distribution was obtained as well, as reported in Figure 5A for the seventh day of growth. It is noticeable the significant change of the cell mass distribution between the first day and the seventh day. Thus, by applying this model the trend of the cell mass distribution over time is predicted for each day of the culture (Figure 5B). To the best of our knowledge, such capability to represent accurately the experimental data of cell number density and of cell mass distribution over time in PBRs was not obtained in previous contributions available in literature. In fact, similar models[11] were validated only using data of biomass concentration (g L^{-1}), but not compared with data of cell number density and of cell mass distributions.

Numerical simulations were also performed for the batch PBR with a higher irradiance, namely at 350 μmol m^{-2} s^{-1}, and compared with experimental results. This irradiation value is over the photosaturation point for *S. obliquus*,[21] where photoinhibition phenomena occur and cells are stressed. Accordingly, to simulate these conditions through the PBE model, some of the model parameters were modified, as reported in Table 1, to account for the effect of higher irradiation. Specifically, the values of E_a and bE_s were chosen according to Bertucco et al.,[23] and k_p was modified according to Sforza et al.[34] who observed an increased maintenance energy requirement under high irradiances.

In the case at 350 μmol m^{-2} s^{-1}, a relationship between m_c and the average cell mass $\langle m \rangle$ was not available, because the required continuous reactor experiments were performed only at 150 μmol m^{-2} s^{-1}. Therefore, constant values of m_c equal to 300 pg and ε equal to 200 pg were used in the simulations at 350 μmol m^{-2} s^{-1} to fit the experimental data of

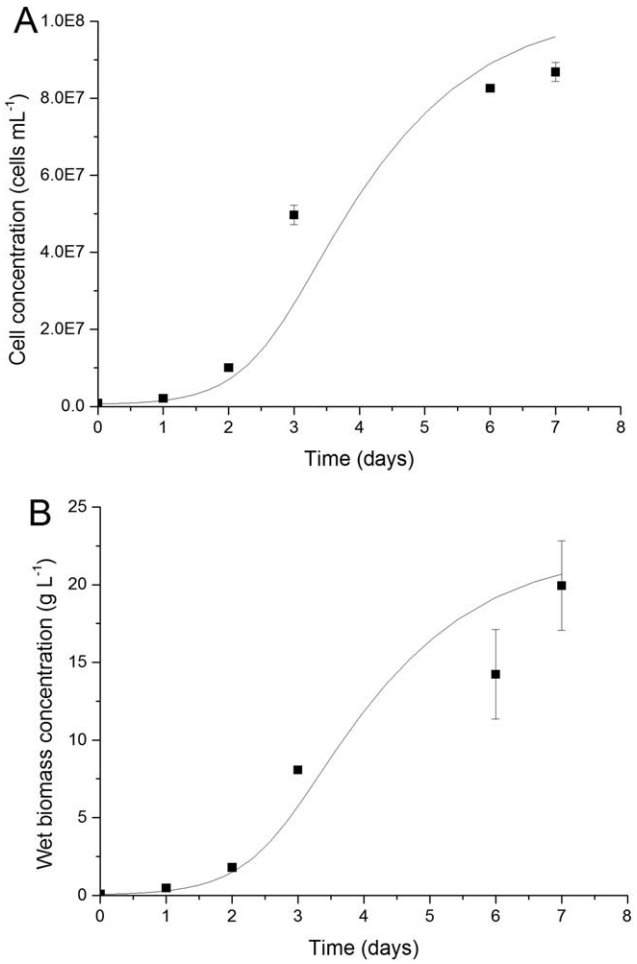

Figure 6. Cell (A) and wet biomass (B) concentrations for *S. obliquus* in batch experiment carried out under 350 μmol of photons m^{-2} s^{-1}.

Squares represent the experimental data, while solid lines are the results of the PBE model.

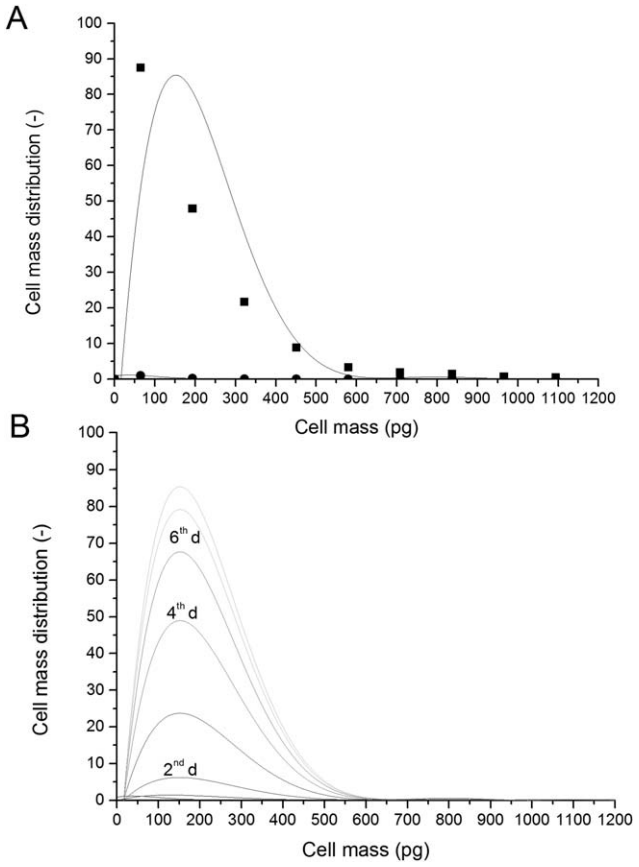

Figure 7. In Figure 7A experimental cell mass distribution of the first (dots) and seventh (squares) day of growth of *S. obliquus* in batch experiment carried out under 350 μmol of photons m^{-2} s^{-1}, compared with the simulated ones (solid lines) are reported.

Figure 7B shows the simulated distribution of cell mass up to eighth day.

wet biomass concentration and cell number density over time. Again, the simulation results show that the proposed PBE model is capable to reproduce satisfactorily the batch experimental data of cell number density and of wet weight (Figures 6A and B), by accounting also for the effect of different light intensities.

On the other hand, the cell mass distribution, shown in Figure 7, reproduces less accurately the experimental data at 350 μmol m^{-2} s^{-1} with respect to the case at 150 μmol m^{-2} s^{-1}, probably due to the effect of the high irradiance and the complexity of the physiological acclimation of photosynthetic organisms under changing environmental conditions. In fact, in the batch experiments performed in this work, the preinoculum was cultivated under low irradiances (about 100 μmol m^{-2} s^{-1}) and, consequently, cells are initially adapted to this operative condition. By exposing the inoculum at higher irradiances, at the beginning of the batch experiment cells are forced to adapt to the new culture condition, and this may strongly influence the trend of the growth curve, affecting also the cell mass distribution. In few days, cells acclimate to high irradiances by increasing their mass. This physiological acclimation is not accounted for in the PBE model, but the experimental data are still reasonably reproduced using m_c equal to 300 pg and ε equal to 200 pg, suggesting that a relation between light intensity and division mass/cell mass might exist, as qualitatively observed in Gris et al.[21]

However, even though the model can be improved to account for the effect of photosaturating and inhibiting intensities, the possibility to integrate the PBE approach with the information on the light availability in a PBR is promising, because light is the main factor affecting the productivity of an algal culture. In fact, by taking into account the light attenuation profile along the depth of the photobioreactor (Eq. 6) according to the model proposed by Pruvost et al.,[30] the mathematical model used in this work is capable to simulate both the effect of light intensity on the cell growth rate and the effect of the increasing biomass concentration (computed from the dimensionless moments at each time) on the light spatial distribution within the PBR. The PAR (I_{dir}) profiles along the reactor depth are shown in Figure 8 for both irradiances and are varying each day as a function of the biomass concentration.

Conclusions

In this work, the growth of *S. obliquus* was both experimentally investigated and modeled by a PBE, accounting for the light radiation effect on cell growth, and for the spatial light distribution. A nice agreement between the experimental data and the simulation results was obtained, in both batch and continuous reactors, under different light intensities. The PBE model, which was thoroughly validated with the experimental results, is capable to reproduce not only the wet biomass concentration but also the cell number density and the cell mass distribution data. Two parameters of the distribution of division mass (m_c and ε) were tuned to fit the experimental data of the continuous experiments at different residence times. In particular, m_c was found to be a function of the residence time, and a relationship between m_c and the average cell mass was proposed, which was shown to be effective also when simulating batch experiments carried out under the same light intensity.

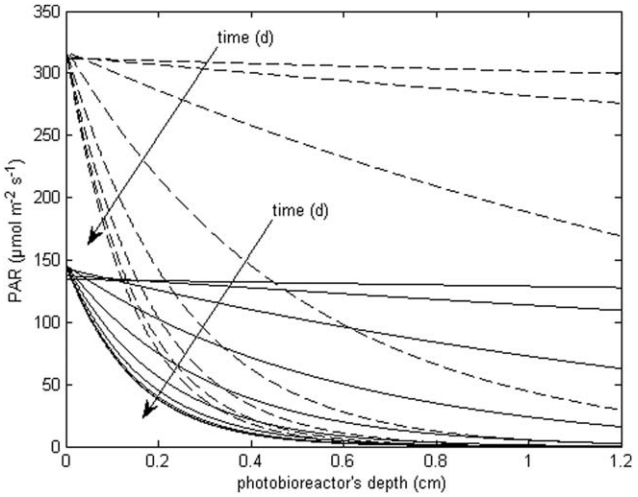

Figure 8. Light intensity profiles along the depth of the batch reactor for each day of growth (indicated by the arrows), for both 150 (solid lines) and 350 (dashed) μmol of photons m^{-2} s^{-1}.

Literature Cited

1. Maity JP, Bundschuh J, Chen C-Y, Bhattacharya P. Microalgae for third generation biofuel production, mitigation of greenhouse gas emissions and wastewater treatment: Present and future perspectives—A mini review. *Energy*. 2014;78(15):104–113.
2. Ho S-H, Ye X, Hasunuma T, Chang J-S, Kondo A. Perspectives on engineering strategies for improving biofuel production from microalgae—A critical review. *Biotechnol Adv*. 2014;32(8):1448–1459.
3. Chisti Y. Constraints to commercialization of algal fuels. *J Biotechnol*. 2013;167(3):201–214.
4. Alberghina L, Ranzi BM, Porro D, Martegani E. Flow cytometry and cell cycle kinetics in continuous and fed-batch fermentations of budding yeast *Biotechnol Prog*. 1991;7(4):299–304.
5. Müller S, Harms H, Bley T. Origin and analysis of microbial population heterogeneity in bioprocesses. *Curr Opin Biotechnol*. 2010;21(1):100–113.
6. Lencastre Fernandes R, Carlquist M, Lundin L, et al. Cell mass and cell cycle dynamics of an asynchronous budding yeast population: experimental observations, flow cytometry data analysis, and multi-scale modeling. *Biotechnol Bioeng*. 2013;110(3):812–826.
7. Eakman JM, Fredrickson AG, Tsuchiya HH. Statistics and dynamics of microbial cell populations. *Chem Eng Prog Symp Ser*. 1966;62:37–49.
8. Davey HM, Kell DB. Flow cytometry and cell sorting of heterogeneous microbial populations : the importance of single-cell analyses. *Microbiol Rev*. 1996;60(4):641–696.
9. Ramkrishna D, Singh MR. Population balance modeling: current status and future prospects. *Annu Rev Chem Biomol Eng*. 2014;5:123–146.
10. Ramkrishna D. *Population Balances. Theory and Applications to Particulate Systems in Engineering*. San Diego: Academic Press, 2000.
11. Concas A, Pisu M, Cao G. Novel simulation model of the solar collector of BIOCOIL photobioreactors for CO2 sequestration with microalgae. *Chem Eng J*. 2010;157(2–3):297–303.
12. Rading MM, Engel TA, Lipowsky R, Valleriani A. Stationary size distributions of growing cells with binary and multiple cell division. *J Stat Phys*. 2011;145(1):1–22.
13. Son S, Tzur A, Weng Y, et al. Direct observation of mammalian cell growth and size regulation. *Nat Methods*. 2012;9(9):910–912.
14. Enfors S, Jahic M, Rozkov A, Xu B, Hecker M, Ju B. Physiological responses to mixing in large scale bioreactors. *J Biosci Bioeng*. 2001;85(2):175–185.
15. Morchain J, Gabelle J, Cockx A. A coupled population balance model and CFD approach for the simulation of mixing issues in lab-scale and industrial bioreactors. *AIChE J*. 2014;60(1):27–40.
16. Hu Q, Sommerfeld M, Jarvis E, et al. Microalgal triacylglycerols as feedstocks for biofuel production: perspectives and advances. *Plant J*. 2008;54(4):621–639.
17. Carvalho AP, Silva SO, Baptista JM, Malcata FX. Light requirements in microalgal photobioreactors: an overview of biophotonic aspects. *Appl Microbiol Biotechnol*. 2011;89(5):1275–1288.
18. Altimari P, Pagnanelli F, Toro L, Chimica D, Sapienza U, Moro PA. Application of structured population balance model for the numerical simulation of a continuous photobioreactor. *Chem Eng Trans*. 2013;32:1027–1032.
19. Travieso L, Hall DO, Rao KK, Benitez F, Sanchez E, Borja R. A helical tubular photobioreactor producing Spirulina in a semicontinuous mode. *Int Biodeterior Biodegrad*. 2001;47:151–155.
20. Strumendo M, Arastoopour H. Solution of PBE by MOM in finite size domains. *Chem Eng Sci*. 2008;63(10):2624–2640.
21. Gris B, Morosinotto T, Giacometti GM, Bertucco A, Sforza E. Cultivation of Scenedesmus obliquus in photobioreactors: effects of light intensities and light-dark cycles on growth, productivity, and biochemical composition. *Appl Biochem Biotechnol*. 2014;172(5):2377–2389.
22. Tang D, Han W, Li P, Miao X, Zhong J. CO2 biofixation and fatty acid composition of Scenedesmus obliquus and Chlorella pyrenoidosa in response to different CO2 levels. *Bioresour Technol*. 2011;102(3):3071–3076.
23. Bertucco A, Beraldi M, Sforza E. Continuous microalgal cultivation in a laboratory-scale photobioreactor under seasonal day-night irradiation: experiments and simulation. *Bioprocess Biosyst Eng*. 2014;37(8):1535–1542.
24. Solana M, Rizza CS, Bertucco A. Exploiting microalgae as a source of essential fatty acids by supercritical fluid extraction of lipids: comparison between Scenedesmus obliquus, Chlorella protothecoides and Nannochloropsis salina. *J Supercrit Fluids*. 2014;92:311–318.
25. Feijó Delgado F, Cermak N, Hecht VC, et al. Intracellular water exchange for measuring the dry mass, water mass and changes in chemical composition of living cells. *PLoS One*. 2013;8(7):e67590.
26. Pottier L, Pruvost J, Deremetz J, Cornet J-F, Legrand J, Dussap CG. A fully predictive model for one-dimensional light attenuation by Chlamydomonas reinhardtii in a torus photobioreactor. *Biotechnol Bioeng*. 2005;91(5):569–582.
27. Cooke R, Kuntz ID. The properties of water in biological systems. *Annu Rev Biophys Bioeng*. 1974;3:95–126.
28. Mantzaris NV. Transient and asymptotic behaviour of the binary breakage problem. *J Phys A Math Gen*. 2005;38(23):5111–5132.
29. Hjortso M. *Population Balances in Biomedical Engineering*. New York: McGraw Hill Professional, 2005.
30. Pruvost J, Van Vooren G, Le Gouic B, Couzinet-Mossion A, Legrand J. Systematic investigation of biomass and lipid productivity by microalgae in photobioreactors for biodiesel application. *Bioresour Technol*. 2011;102(1):150–158.
31. Sforza E, Enzo M, Bertucco A. Design of microalgal biomass production in a continuous photobioreactor: an integrated experimental and modeling approach. *Chem Eng Res Des*. 2014;92(6):1153–1162.
32. Ruiz-Martinez A, Martin Garcia N, Romero I, Seco A, Ferrer J. Microalgae cultivation in wastewater: nutrient removal from anaerobic membrane bioreactor effluent. *Bioresour Technol*. 2012;126C:247–253.
33. Zijffers J-WF, Schippers KJ, Zheng K, Janssen M, Tramper J, Wijffels RH. Maximum photosynthetic yield of green microalgae in photobioreactors. *Mar Biotechnol (NY)*. 2010;12(6):708–718.
34. Sforza E, Urbani S, Bertucco A. Evaluation of maintenance energy requirements in the cultivation of Scenedesmus obliquus: effect of light intensity and regime. *J Appl Phycol*. doi:10.1007/s10811-014-0460-x.
35. Sforza E, Ramos-Tercero EA, Gris B, Bettin F, Milani A, Bertucco A. Integration of Chlorella protothecoides production in wastewater treatment plant: from lab measurements to process design. *Algal Res*. 2014;6(B):223–233.

Manuscript received Dec. 6, 2014, and revision received Apr. 22, 2015.